Role of Magnetic Induction Currents in Nanoslit Excitation of Surface Plasmon Polaritons

Seung-Yeol Lee,[1] Il-Min Lee,[1] Junghyun Park,[1] Sewoong Oh,[1] Wooyoung Lee,[1] Kyoung-Youm Kim,[2] and Byoungho Lee[1,*]

[1]National Creative Research Center for Active Plasmonics Application Systems, Inter-University Semiconductor Research Center and School of Electrical Engineering, Seoul National University, Seoul 151-774, Korea

[2]Department of Optical Engineering, Sejong University, Seoul 143-747, Korea

(Received 7 November 2011; published 25 May 2012)

We present a method for exciting surface plasmon polaritons (SPPs) caused by a magnetic field component perpendicular to the direction of slit. The excitation mechanism is based on the spatially oscillating induced current along the edges of the slit under obliquely incident electromagnetic waves. Our finding distinguishes itself from previous mechanisms based on transverse electric fields and unveils the missing point of the SPP-excitation problem in a nanoslit. The use of a magnetic field for SPP excitation can be highly efficient and even comparable to that with an electric field, so that their composition can lead to selective unidirectional excitation.

DOI: 10.1103/PhysRevLett.108.213907 PACS numbers: 42.25.Ja, 41.20.Jb, 42.82.Et, 73.20.Mf

Light scattering by metallic structures to excite surface plasmon polaritons (SPPs) has attracted significant interest due to their proven potential in nanophotonics [1]. Since the discovery of extraordinary optical transmission (EOT) [2], the fundamental physics underlying this has been extensively researched, resulting in a large body of theoretical work and practical suggestions [3–7]. The pursuit of understanding the basic physics has prompted researchers to focus on elemental subwavelength structures such as an isolated single hole or slit [3–5].

For the slit excitation problems, most previous research has focused on the mechanism of SPP excitation with the incident electromagnetic waves having electric fields perpendicular to the slit. This is because the SPPs are basically collective oscillations of free charges on a metal surface and we thus need an electric field component which is parallel to the direction of propagation of the SPPs (normal to the slit edge) [5–9]. On the other hand, little attention has been paid to the response of a parallel electric field (or perpendicular magnetic field) to the slit, since this state does not have any electric field normal to the slit. Since there is no electric field component to accumulate charge across the slit, previous explanations such as electric dipoles cannot be immediately applied.

However, as we will see, under certain conditions, SPPs can be excited via an incident electromagnetic field that has no electric component normal to the slit. In this situation, the magnetic induction current is the origin of the SPP excitation. On the role of the magnetic fields in metal structures, our work is different from those on the magnetic polaritons [10]. The magnetic polaritons are based on the (effective) negative permittivity mainly induced from the periodicity of the artificial ''magnetic atom'' rather than on the SPP itself. The purpose of this Letter is, with the well-known electric dipole excitations, to provide a comprehensive understanding of the SPP excitation mechanism from a single subwavelength metal slit: our contribution reveals the role of a magnetic induction current in SPP excitation.

For the role of magnetic induction or a magnetic field, we focus on the spatially changing phase profile of a magnetic field caused by an oblique incidence, which creates sinusoidal induction currents along the slit direction. In this Letter, we present an analytic model that sequentially connects the induction currents to the surface charge distribution and the amount of SPP excitation. The proposed model is then confirmed by both a rigorous numerical analysis [11] and an experimental proof. Interestingly enough, the excitation efficiency of the SPPs from perpendicular magnetic fields is comparable to that from conventional perpendicular electric fields. An experimental comparison is done by observing the interference characteristics of both SPPs, which finally leads to the unidirectional launching method of SPPs controlled by polarization modulation.

We consider a single slit in a metal film, illuminated obliquely by a monochromatic plane wave [Fig. 1(a)]. Here, the plane of incidence is parallel to the direction of the slit (on the y-z plane). Regardless of the polarization state, the directions of excited SPPs propagating away from the slit edges are oblique [Fig. 1(a)] so as to match the momentum conservation relation of $k_{\mathrm{SPP}} = k_y/\sin\theta_{\mathrm{SPP}}$, where $k_y = 2\pi/\lambda_y = 2\pi\sin\theta_{\mathrm{inc}}/\lambda$, $k_{\mathrm{SPP}} = k_0[(\varepsilon_{\mathrm{air}}\varepsilon_{\mathrm{metal}})/(\varepsilon_{\mathrm{air}} + \varepsilon_{\mathrm{metal}})]^{1/2}$. Here, ε denotes the relative permittivity and θ_{SPP} is the launching angle of SPPs measured from the normal direction of the slit ($\pm$ x-direction).

Without any loss of generality, we decompose the incident electromagnetic waves into two orthogonal polarization states: TM [magnetic field ($\vec{H}$) is normal to y-z plane] and TE (electric field ($\vec{E}$) is normal to y-z plane], as shown in Fig. 1(a). To prevent unwanted effects such as

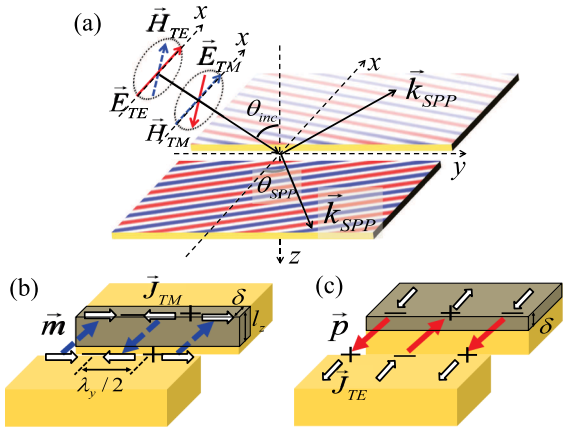

FIG. 1 (color online). (a) The configuration of the system studied. The SPP field distributions are illustrated on the metal surface. The incident wave vector of the plane wave is always laid on the y-z plane so it does not break symmetry with respect to the slit structure. The surface currents ($\vec{J}$), accumulated charges, and induced dipole moments ($\vec{m}$, $\vec{p}$) are illustrated for (b) TM wave and (c) TE wave incidence.

Fabry-Perot resonance inside the slit, we assume a half-infinite thickness for the metal in a theoretical analysis. We also assume that the slit width is sufficiently thin so there is no guided mode excited by the TM incidence.

Let us begin with the case of TM incidence [Fig. 1(b)]. Considering oblique incidence, the protrusion of incident magnetic fields into the nanoslit has sinusoidal oscillations with the period λ_y. Such oscillations can generate a y-directional induction current $\vec{J}_{\mathrm{TM}}$ at the metal surface on the slit wall.

In this picture, the slit walls can be regarded as double parallel wires of which the effective dimension for one side is depicted as a shadowed region in Fig. 1(b). Assuming the currents are uniformly flowing in the effective region, these parallel wires could be replaced by a line distribution of periodically oscillating magnetic dipole sources located at the center of slit. The magnitude of this can be expressed as (see the Supplemental Material [12])

$$|\vec{m}| = |\vec{J}_{\mathrm{TM}}|\delta\frac{\lambda_y}{2\pi}l_z^2, \tag{1}$$

where δ and l_z denote the skin depth from the surface of the slit wall and the effective penetration depth from the surface of the slit walls, respectively.

By assuming that the amplitude of the magnetic field induced by $\vec{m}$ is equal to that of the protruding incident magnetic fields near the slit edge, we have a direct relation between the incident magnetic field $\vec{H}_{\mathrm{inc}}$ and $\vec{J}_{\mathrm{TM}}$ as $\vec{J}_{\mathrm{TM}} = (\tau/\delta)\vec{H}_{\mathrm{inc}}(1 - r_p)\exp(ik_y y)\hat{y}$, where r_p is the Fresnel reflection coefficient for p polarization [13], and $\tau = 4\pi^2(w/2)^3/(\lambda_y l_z^2)$, where w is the width of the slit. Note that the magnitude of τ is approximately in the order of unity for the case of a subwavelength slit.

With $\vec{J}_{\mathrm{TM}}$ at the slit wall, it becomes possible to obtain the magnitude of the oscillating charges near the slit edge from the charge conservation relation as (see the Supplemental Material [12])

$$\sigma_{\mathrm{TM}} = \frac{\lambda}{2\pi c}k_0\delta\tau H_{\mathrm{inc}}(1 - r_p)\sin\theta_{\mathrm{inc}}\exp(ik_y y), \tag{2}$$

where c is the speed of light in free space. This result indicates that, even though there is no charge accumulation between the slit gaps, there exist an amount of oscillating charges near the slit edge caused by TM incidence.

For TE incidence [Fig. 1(c)], the amount of the induced surface currents can be obtained as $\vec{K}_{\mathrm{TE}} = \vec{H}_{\mathrm{inc}}\cos\theta_{\mathrm{inc}}(1 - r_s)\exp(ik_y y)\hat{x}$, by using the surface boundary condition $\vec{K}_{\mathrm{TE}} = \hat{n} \times \vec{H}_{\mathrm{inc}}$ directly at $z = 0$ plane. From this, we can obtain accumulated surface charge densities at each side of the slit as

$$\sigma_{\mathrm{TE}} = \pm\frac{\lambda}{i2\pi c}H_{\mathrm{inc}}(1 - r_s)\cos\theta_{\mathrm{inc}}\exp(ik_y y). \tag{3}$$

The plus and minus signs associated with the charge density are for the left ($x < 0$) and right ($x > 0$) sides of the slit, respectively.

This sign difference, which is not shown in Eq. (2), denotes the fact that the polarities of the charges at each side of the slit are opposite. Therefore, from Eqs. (2) and (3), the parity of the oscillating charges near the slit edge is symmetrical for TM incidence but anti symmetrical for TE incidence.

In Fig. 2(a), the ratio of the accumulated surface charge densities $|\sigma_{\mathrm{TM}}/\sigma_{\mathrm{TE}}|$ and the phase difference $\Delta\varphi = \angle(\sigma_{\mathrm{TM}}/\sigma_{\mathrm{TE}})$ are compared with the amplitude and phase ratio of the surface electric field calculated from a full numerical method of rigorous coupled wave analysis (RCWA) [11], respectively. The match for the entire range of incidence angles shows that the oscillation of surface charges is directly related to the amount of excited SPPs, as has been confirmed in the literature [3–5].

The symmetrical and antisymmetrical charge distributions shown in Eqs. (2) and (3) generate SPPs that possess a symmetrical and antisymmetrical field profile for TE and TM incidence, respectively. These characteristics are shown in Fig. 2(b). In Fig. 2(b), the fields radiating from the electric and magnetic dipoles using Green's function formulation [14,15] based on our analysis are compared with the numerical results (RCWA). Here, we use a magnetic dipole source for the TM incidence obtained by simply adding the phase term in Eq. (1) as expressed in $\vec{m} = |\vec{m}|\exp(i2\pi y/\lambda_y)\hat{x}$, whereas the electric dipole source $\vec{p}$ used for TE incidence is obtained directly from Eq. (3) by $\vec{p} = \sigma_{\mathrm{TE}}w\hat{x}$. The calculations were performed at 2 nm above the half-infinite metal with the following condition: $\lambda = 532$ nm, $\varepsilon_{\mathrm{air}} = 1$, $\varepsilon_{\mathrm{Ag}} = -10.19 + 0.83i$, and $w = 100$ nm. For further descriptions of Green's function analysis, see the Supplemental Material [12]. As can

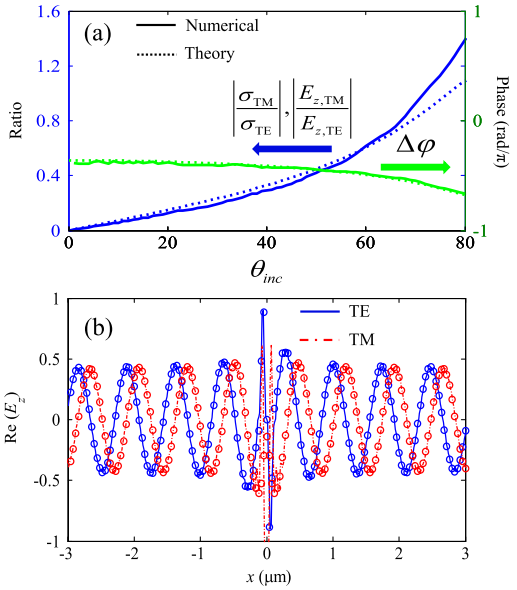

FIG. 2 (color online). (a) Incident angle dependent ratios of induced charge densities (dotted line, theoretical) and E_z fields (solid line, numerical). (b) The E_z field profiles at an incident angle of 50° from numerical (lines) and analytical (Green's dyadic function, markers) methods. The amplitudes of the data are normalized in order to achieve a clear comparison.

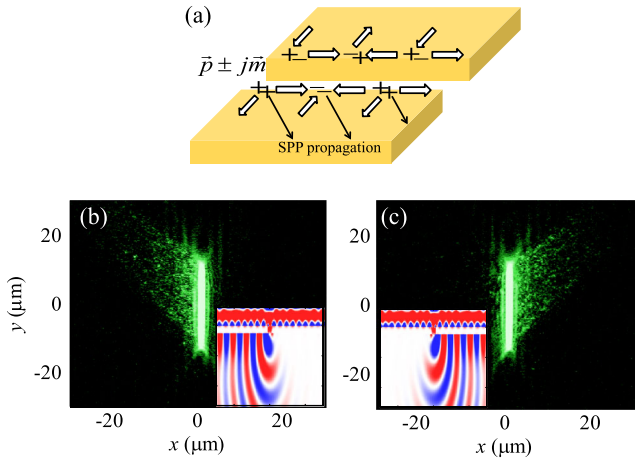

FIG. 3 (color online). (a) Schematic diagram for the unidirectional launching of SPPs done by the composition of TM and TE incidences. Experimental CCD image for unidirectional condition: (b) right-handed (RCP) and (c) left-handed circular polarized (LCP) light incidence with $\theta_{inc} = 50°$ provides left and right side SPP excitation, respectively. Insets show the respective simulation results for the E_z field profile along x-z plane at optimized unidirectional conditions.

be seen from these results, the analytical calculations based on our dipole model are in excellent agreement with the numerical results.

Since charge and field parity induced by the TE and TM incidences are opposite, as shown in Fig. 2, the resulting excitations of SPPs for each side of the slit for these two polarizations will operate in opposite ways. As illustrated in Fig. 3(a), if we illuminate a light with a superposed polarization state of TE and TM, the surface charges near the slit can be accumulated only for one side, whereas those for the other side would be canceled. If we precisely match the amplitude and phase of the incident light, unidirectional excitation of SPPs can be achieved. This can be satisfied if the incident polarization state follows the condition expressed in the Jones vector [16]: $(A_{TE}, A_{TM}) = [|\sigma_{TM}|, \pm|\sigma_{TE}|\exp(-i\Delta\varphi)]$ (left-side enhancement for the + sign). Therefore, it is possible to compare the excitation efficiency of SPPs caused by TM and TE polarization states (which are proportional to $|\sigma_{TM}|$ and $|\sigma_{TE}|$, respectively) by finding the condition for unidirectional launching. According to the results shown in Fig. 2(a), the phase difference for the induced charges between TE and TM cases is found near the value $\Delta\varphi = -\pi/2$, which produces a unidirectional condition near the circularly polarized light when the condition $|\sigma_{TM}| \simeq |\sigma_{TE}|$ is satisfied.

To validate our analysis, an experimental demonstration of the unidirectional excitation of SPPs was carried out. The intensity of the transmitted field captured by a charge-coupled device (CCD) at unidirectional launching conditions is shown in Figs. 3(b) and 3(c). In the insets, we show the RCWA results which are done at the optimized unidirectional launching condition of $(A_{TE}, A_{TM}) = (1, +1.09\angle 77°)$ and $(A_{TE}, A_{TM}) = (1, -1.09\angle 77°)$ for Figs. 3(b) and 3(c), respectively. We use a green laser source ($\lambda = 532$ nm) with an incidence angle of $\theta_{inc} = 50°$. Other geometrical parameters such as the slit width, slit length, and the thickness of the metal (Ag) substrate are fixed at 200 nm, 25 μm, and 120 nm, respectively. These values are designed to provide the ratio of induced charge $|\sigma_{TM}|/|\sigma_{TE}|$ so as to have a unity value at $\theta_{inc} = 50°$. To illuminate the appropriate polarization state for unidirectional launching, we use half-wave and quarter-wave retarders for generating arbitrary polarization states, which are precisely measured by means of a polarimeter module (Thorlabs PAN5710VIS) before illuminating the sample.

In this experiment, the finite thickness of the metal film is unavoidable in contrast to the analytical results. Moreover, it is quite difficult to perfectly separate the reflected near-field from the incident plane wave. Therefore, we measured the transmitted fields from the slit with finite thickness. However, all the conditions were carefully designed so as to maintain the physics laid out in the theoretical analysis. For analytical simplicity, the slit width was chosen to cut off any guided mode for TM incidence and the thickness of the metal was chosen to be thicker than the skin depth to avoid any couplings between the SPPs at the upper and lower surfaces. However, for the efficient generations of $\vec{m}$, non-negligible $\vec{H}_{inc}$ is needed in the slit. Therefore, the slit width and the thickness of the metal are chosen to ensure that a sufficient amount of $\vec{H}_{inc}$ leaks into the slit via attenuating protrusion

of the cutoff modes. As a consequence, it can be assumed that the magnetic dipoles for exciting the SPPs at the bottom surface of the metal film are induced simply by the incident field at that location.

To find the unidirectional launching condition and its efficiency, we plotted the unidirectional ratio (U) in Fig. 4 with the variation in the polarization ellipticity χ. In the numerical result and the experiments, U is defined as the ratio of the intensity of the SPPs excited on the left-side of the slit ($|E_L|^2$) compared to that for the right-side ($|E_R|^2$). We also compared these results with the analytic form

$$U = \frac{|\sigma_{\mathrm{TM}} A_{\mathrm{TM}} - \sigma_{\mathrm{TE}} A_{\mathrm{TE}}|^2}{|\sigma_{\mathrm{TM}} A_{\mathrm{TM}} + \sigma_{\mathrm{TE}} A_{\mathrm{TE}}|^2}, \tag{4}$$

where the numerator and denominator denote the amount of excited SPPs at the left and right side of the slit, respectively.

By gradually changing the polarization state through TE, RCP, TM, LCP, and back to the TE state, the results show that the highest unidirectional ratio is obtained near the RCP state, whereas the inverse peak is located near the LCP state as predicted by our analytic model. We used the magnitude of σ_{TM} and σ_{TE} based on Eqs. (2) and (3), whereas their phases were extracted from the numerical results, since the phase of the oscillating charge can be perturbed by multiple reflections inside the finite thickness of the metal slit. However, these phase perturbations have no effect on the location of the peaks, but do affect their sharpness. The location of the peaks is only sensitive to the ratio of the amplitudes $|\sigma_{\mathrm{TM}}/\sigma_{\mathrm{TE}}|$.

It can be expected from Eq. (4) that it is necessary to satisfy the condition $|\sigma_{\mathrm{TM}}/\sigma_{\mathrm{TE}}| = 1$ to create the unidirectional launching condition near the RCP and LCP states. Therefore, from Fig. 4, we also know that the scale of the excitation efficiency of SPPs caused by TM incidence is comparable to that caused by TE incidence, which constitutes experimental proof of our findings.

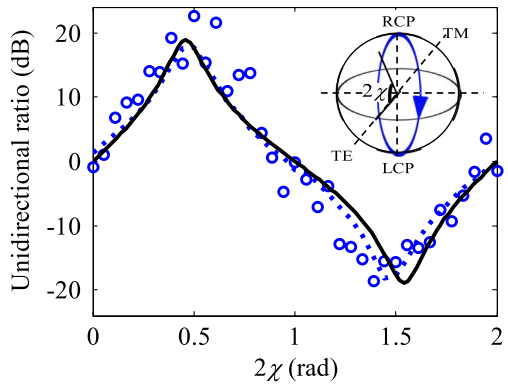

FIG. 4 (color online). Experimentally measured (marker) and numerically calculated (dotted blue line) left-to-right SPP launching ratios are compared with the theoretical plot (solid black line) varying with the incident polarization state. The polarization elipticity χ is changed along the path shown in the Poincaré sphere (inset).

In conclusion, we proposed a mechanism for the excitation of SPPs in a metallic nanoslit by the oblique incidence of light with a perpendicular magnetic field. The origin of this excitation is the sinusoidal variation of the induction current near the slit edges. Remarkably, the excitation efficiency of the excited SPPs by TM incidence is sufficiently strong that it approaches the level of that by TE incidence. Furthermore, a novel unidirectional launching mechanism of SPPs has been suggested and demonstrated by experiment. This type of unidirectional launching also has its own impact, since it efficiently guides the SPP without symmetry breaking in neither geometry nor incident momentum. The selective launching of SPPs from either side of the slit can be achieved by simply changing the polarization state of the incident field. We expect that our study will be helpful for developing a more complete understanding of the nature of SPPs. We also anticipate that the proposed unidirectional SPP launching scheme can be utilized in various types of plasmonic switching devices.

This work was supported by the National Research Foundation and the Ministry of Education, Science, and Technology of Korea through the Creative Research Initiative Program (Active Plasmonics Application Systems).

*byoungho@snu.ac.kr

[1] W. L. Barnes, A. Dereux, and T. W. Ebbesen, Nature (London) **424**, 824 (2003).
[2] T. W. Ebbesen, H. J. Lezec, H. F. Ghaemi, T. Thio, and P. A. Wolff, Nature (London) **391**, 667 (1998).
[3] P. Lalanne and J. P. Hugonin, Nature Phys. **2**, 551 (2006).
[4] A. Y. Nikitin, F. J. Garcia-Vidal, and L. Martin-Moreno, Phys. Rev. Lett. **105**, 073902 (2010).
[5] P. Lalanne, J. P. Hugonin, and J. C. Rodier, Phys. Rev. Lett. **95**, 263902 (2005).
[6] G. Leveque, O. J. F. Martin, and J. Weiner, Phys. Rev. B **76**, 155418 (2007).
[7] A. Yu. Nikitin, F. J. Garcia-Vidal, and L. Martin-Moreno, Phys. Rev. B **83**, 155448 (2011).
[8] Z. Liu, Y. Wang, J. Yao, H. Lee, W. Srituravanich, and X. Zhang, Nano Lett. **9**, 462 (2009); H. F. Schouten, N. Kuzmin, G. Dubois, T. D. Visser, G. Gbur, P. F. A. Alkemade, H. Blok, G. W. 't Hooft, D. Lenstra, and E. R. Eliel, Phys. Rev. Lett. **94**, 053901 (2005).
[9] J. H. Kang, D. S. Kim, and Q.-H. Park, Phys. Rev. Lett. **102**, 093906 (2009).
[10] T. Li, H. Liu, F. M. Wang, J. Q. Li, Y. Y. Zhu, and S. N. Zhu, Phys. Rev. E **76**, 016606 (2007); T. Li, J.-Q. Li, F.-M. Wang, Q.-J. Wang, H. Liu, S.-N. Zhu, and Y.-Y. Zhu, Appl. Phys. Lett. **90**, 251112 (2007).
[11] M. G. Moharam, E. B. Grann, D. A. Pommet, and T. K. Gayload, J. Opt. Soc. Am. A **12**, 1068 (1995); P. Lalanne, J. Opt. Soc. Am. A **14**, 1592 (1997); H. Kim, I.-M. Lee, and B. Lee, J. Opt. Soc. Am. A **24**, 2313 (2007).

[12] See Supplemental Material at http://link.aps.org/supplemental/10.1103/PhysRevLett.108.213907 for the derivation of Eqs. (1)–(3) and detailed Green dyadic analysis.
[13] J. D. Jackson, *Classical Electrodynamics* (Wiley, New York, 1998), 3rd ed.
[14] L. Novotny and B. Hetch, *Principles of Nano-Optics* (Cambridge University Press, New York, 2006).
[15] M. Paulus and O. J. F. Martin, Phys. Rev. E **63**, 066615 (2001).
[16] A. Yariv and P. Yeh, *Optical Waves in Crystals* (Wiley, New York, 1984).